Two-Phase Vessel Blowdown of an Initially Saturated Liquid—Part 1: Experimental

M. N. Hutcherson
Senior Mechanical Engineer.
Assoc. Mem. ASME

R. E. Henry
Vice President.

Fauske & Associates, Inc.
Burr Ridge, Ill. 60521

D. E. Wollersheim
Professor,
Mechanical Engineering Department,
University of Missouri,
Columbia, Mo.

Experimental blowdown results for initially isothermal, saturated water from a small pressure vessel containing internal geometry are presented. This experiment simulated a break in a large duct of approximately three diameters in length which exited from the vessel. Choking only occurred at the exit of the discharge duct, and the instantaneous internal vessel pressure distribution was nearly uniform. Most of the fluid within the vessel immediately after the initiation of the blowdown became superheated liquid. This thermodynamic state together with the activated wall cavities inside the vessel maintained a nearly constant internal vessel pressure history early in the blowdown. However, in the latter stage of the depressurization, the remaining fluid within the vessel was essentially in thermodynamic equilibrium. A nonuniform distribution of fluid quality within the vessel was also detected in this experiment. In addition, this experiment illustrates that transient, two-phase, critical flow in large diameter ducts is similar to steady, two-phase, critical flow in small diameter ducts.

1 Introduction

The critical flow problem which is an integral element in the compressible blowdown phenomenon has been studied by many investigators [1–17]. The two phase critical flow from high pressure-temperature systems has been studied primarily in the steady-state case. However, some transient, two-phase critical flow work [7, 11, 18–26] has also been performed. The two-phase blowdown phenomenon is a subject of great interest to both the chemical and power industries. It is particularly pertinent to fossil-fuel fired, steam-water boilers and pressurized and boiling water nuclear reactor systems. It is also applicable to railway transportation of saturated and subcooled liquids [27]. The critical flow rate at a break in such a system is the controlling flow mechanism for most of the decompression. Hence, the critical flow phenomenon is an essential element in the analysis of the blowdown transient.

It has been shown [11] that the nature of the two-phase decompression phenomenon is strongly affected by (*i*) the configuration of the blowdown vessel, (*ii*) the internal geometry within the vessel, and (*iii*) the break location from the vessel. There has been considerable large-scale blowdown experimentation [11, 18–24, 26] primarily directed toward resolving this issue in light water nuclear reactor safety. A variety of vessel and exhaust duct arrangements have been employed, and the decompressions have been initiated from a spectrum of initial conditions. This particular study has considered a break in an "inlet line" to such a nuclear reactor vessel, and this was experimentally modeled with the apparatus illustrated in Fig. 1. A pipe break at this location in such a system has been considered to create a "worst case" blowdown for primarily two reasons:

1 The fluid entering the vessel is at a lower total temperature than the exiting fluid. Hence, the critical flow rate from an inlet duct is greater than from an outlet duct.

2 A break in an inlet line requires the core flow to stagnate and reverse flow direction in order to exhaust from an inlet duct. This flow stagnation and subsequent reversal may significantly decrease the heat transfer from the core during this period.

In the past, it has often been assumed in analyzing the two-phase decompression of such a system that the instantaneous pressure distribution inside the blowdown vessel is nearly uniform. Thermodynamic equilibrium of the remaining fluid has also been often assumed from the initiation of the blowdown. The fluid quality inside the vessel has been considered to be the isentropic quality in the absence of significant heat transfer. The two-phase critical flow phenomenon has also been assumed to be primarily the same in the transient, large duct case as in the steady-state, small duct case. This permits the models which have been verified against the steady-state, small duct data to be applied in the transient, large duct case as well. Metastable thermodynamic states have also been shown [11, 21, 28–31] to exist at the start of decompression from both saturated and subcooled liquid conditions. Choking inside the blowdown vessel and also at the break from the system is also possible under proper conditions. In reviewing the literature, these were then some of the salient questions on this topic which deserved further study. Hence, the foregoing questions served as the foundation upon which this study was formulated.

In view of the preceding discussion, the objectives of the experimental portion of this investigation [11] were to determine:

1 The effect of internal flow area changes on the possibility of choking occurring within this system

2 The effect that metastable thermodynamic states, primarily superheated liquid, have on the decompression sequence

3 Whether transient, two-phase critical flow in large diameter ducts is sufficiently similar to steady-state, two-phase critical flow in small diameter ducts to justify being modeled in a similar manner

Hence, the objective of this article is to briefly summarize the results of the experimental portion of this study and to support the major findings of the same.

2 Experimental Apparatus

The apparatus employed in this experiment was a cylindrical vessel with a volume of approximately 0.153 m^3 (5.40 $ft.^3$) as illustrated in Fig. 1. It had an attached duct which was 0.108-m (4.257-in.) i.d. and about 0.330-m (13-in.) long, (L/D = 3). This simulated a typical broken inlet duct in a

Contributed by the Heat Transfer Division for publication in the JOURNAL OF HEAT TRANSFER. Manuscript received by the Heat Transfer Division January 12, 1982.

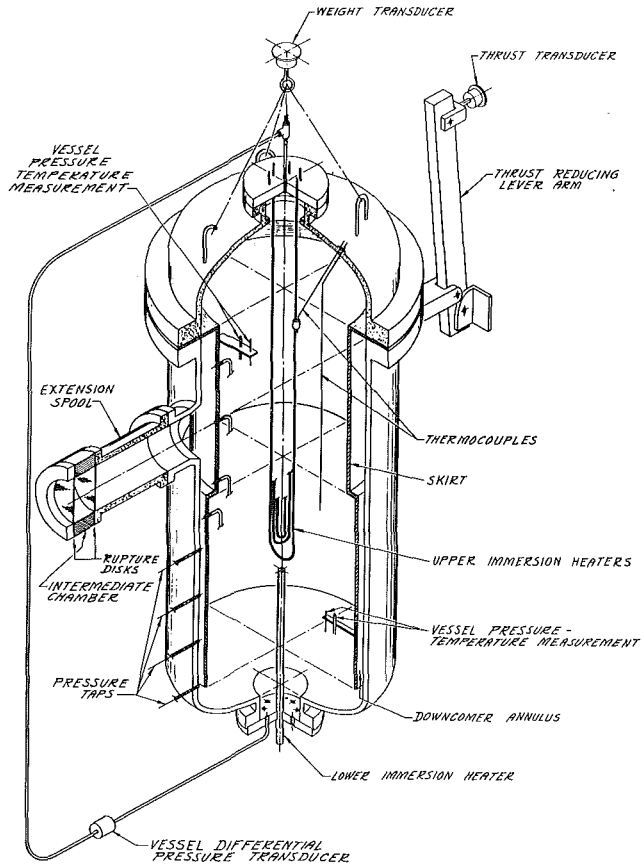

Fig. 1 Schematic of the apparatus employed in this blowdown experiment

pressurized water, nuclear reactor system. A set of two rupture disks was employed at the end of the exhaust duct to contain the fluid during heatup, and they were also used to initiate the decompressions when the desired thermodynamic conditions were established. The vessel also contained internal geometry in the form of a skirt, Fig. 1, which simulated the core barrel in a nuclear reactor vessel. For an inlet line break, the core flow is required to stagnate, reverse, and exhaust up the downcomer annulus and out the broken inlet duct.

The vessel was instrumented with two load cells and various pressure taps and thermocouples, as illustrated in Fig. 1. One of the two load cells measured the weight of the remaining fluid within the vessel, and the other one measured the thrust produced during the blowdown. Both the weight and thrust sensors were 4448 N (1000 lbf) Statham, unbounded strain gage transducers. The total suspended weight of the fluid and vessel when full of 294 K (70°F) water was approximately 2224 N (500 lbf). The maximum thrust produced in this experiment was about 31 KN (7000 lbf), and this was sensed as 3.1 KN (700 lbf) through the 10 to 1 reduction ratio lever arm. The vessel was also instrumented with 15 static pressure taps. All of these taps were 2-mm (1/16-in.) dia, with the exception of two taps near the end of the exhaust duct, P_{14} and P_{15}, which were 1-mm (1/32-in.)-dia taps. Six-mm (1/4-in.) o.d., 5-mm (0.183-in.)-i.d., stainless steel tubing connected each of the pressure taps to an individual pressure transducer. All the pressure transducers were at atmospheric conditions. They were all Statham, strain gage, diaphragm transducers, and their ranges were from 0–4.24 MPa (0–600 psig) to 0–17.2 MPa (0–2500 psig). The smaller range transducers were used to measure the pressures of greatest importance. The hard lines connecting the pressure taps and transduces were filled primarily with water during the blowdown. The longest connecting hard line was 1.12-m (44-in.), and the response time of this line and transducer was about 0.3 ms. This was well within acceptable response for the purpose of this study. There were also 14 chromel-alumel thermocouples employed in this system. Four of these thermocouples were located inside the vessel to measure the local fluid stagnation temperature (T_1, T_2, T_7, T_8), and these were 2-mm (1/16-in.) o.d. sheathed thermocouples, Fig. 1. The remaining 10 temperature sensors were 24 gage, bare wire thermocouples welded onto the exterior wall of the vessel. All the preceding measurements were recorded as analog signals with the exception of the 10 bare wire thermocouples.

3 Discussion

3.1 Calibration Test. A calibration run was performed before executing the reported two-phase tests to ensure the instrumentation was performing properly. The primary concern was with the weight and thrust measurements because of their importance in this study. The exhaust flow rate was determined by differentiating the weight decay measurement, and the thrust measurement also had to be verified. Thus, a

Nomenclature

A = flow area
C = concentration
c = specific heat capacity
D = diameter
F = force, thrust
G = mass flux, $\dot{m}/A$
h = specific enthalpy
K = Henry's concentration coefficient
k = slip ratio, u_V/u_L
m = mass, milli (10^{-3})
$\dot{m}$ = mass flow rate
P = pressure
$_7\bar{P}_8$ = average internal vessel pressure
R = radius
s = second
T = temperature
t = time
u = flow speed
v = specific volume
x = fluid quality
(0) = time zero
α = void fraction
γ = ratio of specific heat capacities, c_p/c_v
η = throat pressure ratio (P_t/P_o or $P_t/P_{T,e}$)
ρ = fluid density
σ = surface tension
τ = arbitrary time

Subscripts

a = ambient, activation
b = bubble
c = critical or choked
d = deactivated
E = thermodynamic equilibrium
e = entrance
f = final
g = noncondensible gas, superheated vapor
h = constant enthalpy
IS = internal skirt
i = initial
L = saturated liquid
l = subcooled liquid
max = maximum
o = stagnation
p = constant pressure
s = constant entropy
sat = saturation
T = total, total thermodynamic property
t = throat
V = saturated vapor
v = constant volume
VL = saturated vapor minus liquid thermodynamic property
x = exit
1 = upstream location, thermodynamic state
2 = thermodynamic state

calibration blowdown was virtually required to validate these measurements. Such a calibration was performed by filling the vessel with 293 K (68°F) water while only leaving a gas space inside the upper region of the internal skirt, Fig. 1. This gas space was then filled with nitrogen gas. This gas then acted against the virtually incompressible water to motivate the blowdown after the rupture disks were broken. The annulus was initially full of water in this configuration, Fig. 1, and the density of the fluid at the exit of the exhaust duct during the blowdown was well known. This enabled a check to be performed on the consistency of the exhaust flow rate. It was evaluated in three ways: (*i*) from the measured remaining weight of fluid, (*ii*) the measured thrust, and (*iii*) the measured total pressure at the entrance to the exhaust duct. The pressure and temperature instrumentation were not really suspect; hence, little effort was directed at them.

The validity of the remaining mass signal was also checked against the predicted thermodynamic extremes of the expansion of the driving nitrogen gas (adiabatic and isothermal). The measured mass followed the isentropic prediction of the nitrogen expansion much more closely than the isothermal prediction particularly at the beginning of the blowdown. The measurements diverged somewhat from the isentropic prediction later in the decompression because of heat transfer from the entrained water droplets to the expanding and cooling nitrogen gas. Hence, the remaining mass measurements were bracketed by the extremes of how the nitrogen gas could have expanded during the decompression. Thus, the measurements were considered realistic. The thrust and internal vessel pressure also were analyzed in the same manner, and similar results were determined. Thus, all the measurements appeared to be realistic and consistent with each other.

The consistency of the measurements of remaining mass, thrust, and the total pressure at the entrance to the exhaust duct were checked in the following manner. This was accomplished by translating the foregoing measurements into a flow rate. The flow rate determined from the measured remaining mass is given by

$$G = \frac{1}{A_x}\frac{dm}{dt} \tag{1}$$

That from the thrust is

$$G = \sqrt{F\rho_l / A_x} \tag{2}$$

and that from the upstream total pressure considering no losses is

$$G = \sqrt{2\rho_l (P_{T,1} - P_a)} \tag{3}$$

The trends in the flow rate derived from these techniques were very similar for most of the calibration decompression. Hence, all the experimental measurements were considered to be reliable and consistent, and the system was then ready for a two phase blowdown.

3.2 Two-Phase Tests. Blowdown characteristics of a system are strongly dependent on the exhaust duct size in relation to the vessel, location of the exhaust duct from the vessel, and also the internal surface area and volume of the vessel. Experiment has shown [32] that at the beginning of subcooled and saturated liquid blowdown, the nucleation process, which is responsible for the creation of the vapor phase, occurs primarily at the interface between the liquid and containing wall rather than in the liquid freestream. In addition, the heat-up history of such a system has a significant affect on the initiation of the nucleation process and subsequent decompression. This is primarily illustrated by how far the internal vessel pressure drops below the local saturation pressure at the start of decompression. An important effect which occurs during heat-up and blowdown initiation is the action within the internal surface wall cavities. The equilibrium radius of a bubble or cavity during heatup can be approximated as

$$R_E = \frac{2\sigma(T)}{P_l - P_b} \tag{4}$$

where P_b is generally the sum of the working fluid vapor pressure, P_V or $P_{\text{sat}}(T)$, and any nonconsiderable gas pressure, P_g. The noncondensable gas pressure can be related to the concentration of that gas as

$$C(P, T) = \mathrm{K}(T) P_g \tag{5}$$

The concentration of noncondensable gases was constant within the vessel in a given test in this experiment, thus

$$P_{g,2} = P_{g,1}\frac{\mathrm{K}(T_1)}{\mathrm{K}(T_2)} \tag{6}$$

Hence, since the heat-up history of pressure and temperature was known, (4) may be used to approximate the largest remaining unflooded wall cavity before blowdown in this experiment as

$$R_{E,d} = \frac{2\sigma(T_d)}{P_{l,d} - \dfrac{\mathrm{K}(T_1)}{\mathrm{K}(T_2)} P_{g,1} - P_{\text{sat}}(T_{l,d})} \tag{7}$$

The largest remaining unflooded wall cavity at blowdown initiation, (4), is the same as that after heatup and is given by

$$R_{E,a} = \frac{2\sigma(T_{l,2})}{P_{\text{sat}}(T_{l,2}) + \dfrac{\mathrm{K}(T_1)}{\mathrm{K}(T_2)} P_{g,1} - P_{l,2}} \tag{8}$$

Equations (7) and (8) can then be combined to yield the superheat (temperature or pressure) required to activate the largest existing surface cavity at the start of decompression. This then is a simple method of yielding the extent to which the internal vessel pressure may drop below the local saturation pressure before sufficient wall cavities are activated to produce adequate vapor volume to in turn increase the vessel pressure. This is illustrated in Fig. 2 where the internal vessel pressure ($_7\bar{P}_8/P_0(0)$) dropped momentarily before recovering toward its plateau value after which it decayed in an equilibrium manner. This method was used in this experiment and produced comparable superheats as those measured at the start of these blowdowns.

The rapid decrease and subsequent recovery of the internal vessel pressure at the start of these decompressions indicate the existence of a metastable thermodynamic state during this period. The metastable decompression regime of the blowdown continued until the remaining fluid within the system became dispersed and thermodynamic equilibrium was closely approached. This is shown in this experiment by considering the two equilibrium extremes of how the remaining fluid could expand during the blowdown (isentropically and isenthalpically). These two equilibrium expansion paths were considered, and the remaining fluid mass was calculated using the measured internal vessel pressure. The calculated remaining mass based on the measured interval vessel pressure agreed with the measured remaining mass at a calculated void fraction in the internal skirt (α_{IS}) of approximately 0.5, Fig. 2. At this time, thermodynamic equilibrium was essentially established because at a void fraction of about 30 percent, a bubbly flow regime normally transactions to a dispersed one with liquid droplets suspended in a vapor continuum [33]. This then generates significant heat transfer surface area, and thus thermodynamic equilibrium is approached. At this point, the internal vessel

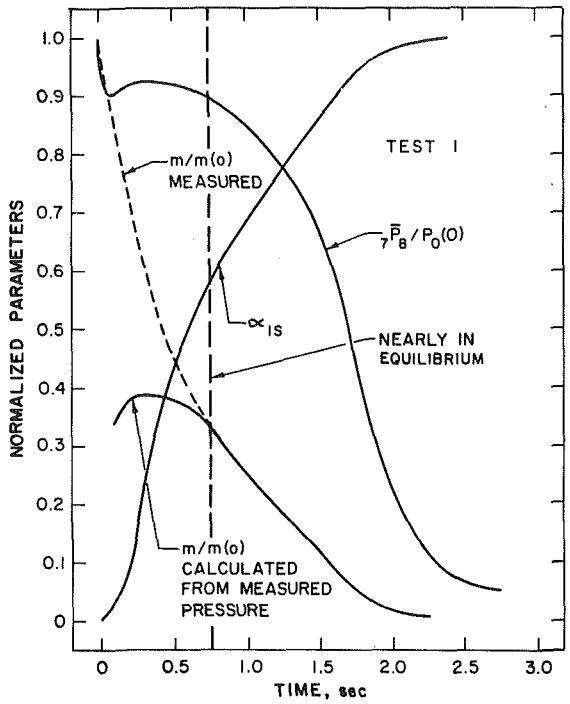

Fig. 2 An indication of when equilibrium of the remaining fluid in the internal skirt region was reached in test 1

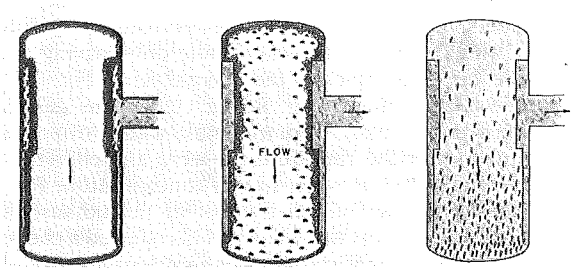

Fig. 3 Schematic of the blowdown vessel illustrating the proposed flow regimes inside the vessel during the various stages of decompression in these tests

pressure also began to decrease from its plateau value as shown in Fig. 2.

The flow regimes which most probably prevailed within this blowdown vessel during the various stages of these decompressions are illustrated in Fig. 3. The indicated time periods when the various flow regimes existed during these blowdowns are applicable to this particular geometry. Almost all the remaining fluid was in a metastable state (superheated liquid) during the first 100 ms. During this time, the surface cavities had been activated and the resulting voids were growing into the superheated liquid. Almost all the fluid within the internal skirt was superheated liquid, and that within the annulus was rapidly becoming a dispersed, two-phase, liquid-vapor mixture.

During this early period, the internal vessel pressure dropped below the saturation pressure and subsequently began to increase toward its plateau value, Fig. 2. The initial drop of the internal vessel pressure below the saturation pressure occurred because there was insufficient volume being produced by the expanding voids. The vapor volume production originating from the surface cavities could not keep pace with the volume expulsion rate. However, after only a short period, sufficient voids had expanded to adequate size to dramatically increase the volume production rate within the vessel. When this exceeded the volume exhaust rate, the internal vessel pressure then began to rise and approach a momentarily constant value, Fig. 2.

From about 100 to 600 ms, the fluid within the annulus was virtually completely dispersed, and the expanding voids originating from the walls were propagating a considerable distance into the superheated liquid within the internal skirt. During this period, the volume production rate within the vessel was approximately equal to the volume exhaust rate from the system. This was indicated by the nearly constant internal vessel pressure, Fig. 2. Once sufficient fluid had been exhausted from the system, the expanding bubbles were nearly uniformly distributed within the liquid remaining in the internal skirt. The resulting two-phase, liquid-vapor mixture was well dispersed, and equilibrium between the remaining liquid and vapor was approached. This is indicated in Fig. 2, where the internal vessel pressure decreased in a nearly equilibrium manner, and the measured and calculated remaining fluid masses agreed. During this period, the fluid volume expulsion rate greatly exceeded the production rate, hence, the internal vessel pressure decreased.

There was no evidence that the flow choked within this vessel, particularly at the annular area enlargement, Fig. 1, during these depressurizations. The pressure upstream and downstream of the annular area enlargement and the internal vessel pressure were all virtually the same. If the flow up the annulus had choked at the area enlargement, the static pressure just upstream of the area enlargement would have only been approximately 75 percent of the internal vessel pressure. The relation between the pressures immediately upstream and downstream of the area enlargement would have depended on the "back pressure" – that pressure immediately upstream of the exhaust duct. The static pressure immediately upstream and downstream of the annular area enlargement were virtually identical, hence, the flow at this location was *not* choked. This was not particularly surprising because the annular area was approximately 2.5 times larger than the exhaust duct area. The only location in this system were the exhausting flow did choke was at the minimum area section, i.e., at the exit of the exhaust duct. Motion pictures of the exhaust plane flow indicated that fully developed critical flow was established approximately 25 ms after the rupture disks had broken. The same motion pictures and the measured critical pressure ratio histories indicated that the exhausting flow was choked for about 70 percent of the 2.5 s decompressions.

The fluid quality at the entrance to the exhaust duct in this experiment deviated considerably from equilibrium conditions. The fluid quality for a uniformly distributed, homogeneous equilibrium, isentropic expansion within the vessel is given by

$$x_s = \frac{s_L(T_o) - s_L(P)}{s_{VL}(P)} \tag{9}$$

and similarly for an isenthalpic expansion

$$x_h = \frac{h_L(T_o) - h_L(P)}{h_{VL}(P)} \tag{10}$$

These two equilibrium, upstream fluid qualities as based on the measured internal vessel pressure are shown in Fig. 4. The fluid quality at the entrance to the exhaust duct was assumed to be approximately the same as at the exit. This is because the static pressure in such a short duct ($L/D = 3$) is nearly constant. Thus, there is virtually no phase change for fluid in residence in such a short length. Each of these two equilibrium fluid qualities, (9) and (10), was employed in an energy balance on the system during the blowdown given by

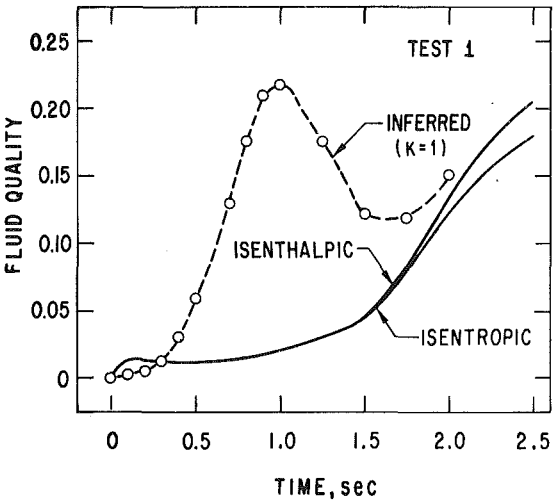

Fig. 4 Comparison of the inferred fluid quality and the entrance isentropic and isenthalpic qualities based on the measured pressure in test 1

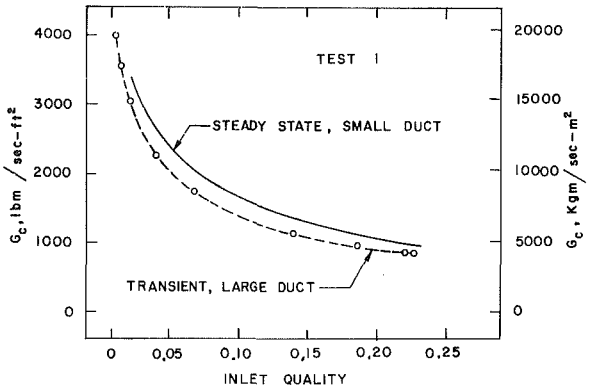

Fig. 5 Comparison of the transient, large duct, critical flow rates in test 1 and the corresponding steady-state, small duct, critical flow rates in [9]

$$m(0)h(0)-m(\tau)h(\tau)=A_x\int_0^\tau G\Big\{[h_V x+h_L(1-x)]+\frac{1}{2}G^2\Big[v_V x+v_L(1-x)\Big]^2\Big\}_x\,dt \tag{11}$$

The measured critical flow rates and the instantaneous pressures were used in (11). The balance employing the isentropic quality (9) was approximately 8 percent low, and the same employing the isenthalpic quality (10) was about 7 percent low. This indicated that the fluid quality at the entrance and exit of the exhaust duct was apparently not an equilibrium value. Fortunately, it was also possible to evaluate the fluid quality at the exit of the exhaust duct by employing a variety of the system measurements. The homogeneous exit specific volume was formulated as

$$v_x=\frac{1}{G_c^2}\left[\frac{F}{A_x}+P_a-P_x\right] \tag{12}$$

and the exit fluid quality was then determined from

$$x_x=\frac{v_x-v_L(P_x)}{v_{VL}(P_x)} \tag{13}$$

Assuming that (*i*) the fluid quality in the duct was approximately constant, (*ii*) the liquid phase was virtually incompressible, and (*iii*) the vapor phase expanded isentropically in the duct, then (13) can be recast as

$$x_1=\frac{v_x-v_L(P_{T,1})}{v_V(P_{T,1})\eta^{-1/\gamma}-v_L(P_{T,1})} \tag{14}$$

This homogeneous inferred inlet quality is also shown in Fig. 4. It is readily apparent that the shape of this inferred inlet quality curve is significantly different than that of the equilibrium qualities. This is an indication of the nonuniformity of the flow pattern within this vessel during these blowdowns. It should be noted in Fig. 4 that the inferred entrance quality began to significantly increase above the equilibrium qualities at approximately 300 ms which was after the annulus had initially been voided, Fig. 3. However, it was during this time period that the vapor phase was probably being swept up the downcomer annulus toward the exhaust duct. This vapor phase was being generated at the lower, inside wall of the internal skirt. The exhaust critical flow rate was also decreasing very rapidly at about this same time. This is consistent since the critical flow rate decreases dramatically for small increases in inlet quality in the low quality regime [9]. This homogeneous inferred inlet quality (14) was then employed in an energy balance on the system (11) to assess its validity. The energy exhausted from the system was determined from using (*i*) the homogeneous inferred inlet quality, (*ii*) the experimental critical flow rates, and (*iii*) the measured internal vessel pressure. These resulting energy balances were then within 1 percent of the initial total energy inventory. This therefore provided good confidence that the homogeneous inferred quality was a valid representation of the actual fluid quality in the exhaust duct during the blowdown.

The case of a nonhomogeneous ($k > 1$) inferred quality was also investigated, and it was determined not to be as realistic as the homogeneous ($k = 1$) case. The nonhomogeneous quality was formulated by combining the continuity equation

$$\dot{m}=\rho_V A_V u_V+\rho_L A_L u_L \tag{15}$$

and a summation of the momentum flow rates of each phase as

$$\dot{m}u=\dot{m}_V u_V+\dot{m}_L u_L \tag{16}$$

This resulted in the nonhomogeneous quality as a function of the velocity ratio (k) as

$$x=\frac{-\left[\frac{v_V}{k}+v_L(k-2)\right]+\left\{\left[\frac{v_V}{k}+v_L(k-2)\right]^2+4(v-v_L)\left[v_V\frac{k-1}{k}-v_L(k-1)\right]\right\}^{1/2}}{2\left[v_V\frac{k-1}{k}-v_L(k-1)\right]} \tag{17}$$

Assumptions (*i*) and (*iii*) that were employed in formulating (14) were also applied in (17). Once this was accomplished and (12) and (17) were combined, the energy exhausted from the system as determined from (11) increased with velocity ratio much above the 1 percent agreement obtained with the homogeneous inferred inlet quality. Thus, the actual exhausting flow was apparently very nearly homogeneous in view of the good energy balance comparison.

The transient, large duct, critical flow rates from this study compare well with the steady-state, small duct, critical flow rates of previous investigators [9], as illustrated in Fig. 5. The steady-state, critical flow rates shown in Fig. 5 are for entrance total pressures of 0.689–6.550 MPa (100-950 psia) and entrance qualities of 0.01–0.2275. These steady-state, critical flow rates were measured in convergent-divergent, axisym-

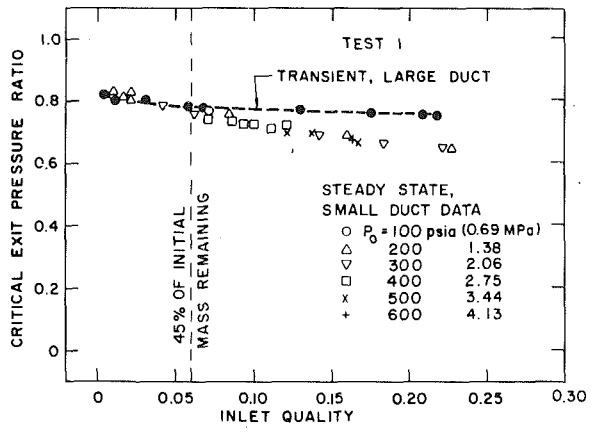

Fig. 6 Comparison of the transient, large duct, critical pressure ratio in test 1 and the steady-state, small duct, critical throat pressure ratio in [9]

metric nozzles with 6.44 and 11.1-mm (0.253 and 0.438-in.)-dia. throats. For comparison, the i.d. of the constant area exhaust duct in this study was 0.108-m (4.257-in.). The average difference between these two sets of two phase critical flow rate data is about 19 percent with the transient, large duct critical flow rates being less than the steady-state, small duct critical flow rates. The same good agreement was true of test 2 in this experiment. Based on this critical flow rate data comparison, the critical flow phenomenon appears to be quite similar in the transient, large duct and steady-state, small duct cases, as has also been inferred in [23, 25, 26].

The transient, large duct, critical exit pressure ratios from this study also compare well with steady-state, small duct, critical throat pressure ratios [9], as illustrated in Fig. 6. These two sets of critical pressure ratio data are virtually identical up to an inferred inlet quality of approximately 6 percent. At this point, less than half the initial fluid remained within the vessel during these blowdowns, Figs. 2 and 6. This was also after the critical flow rate had decreased to approximately 9800 Kgm/s-m^2 (2000 lbm/s-ft^2), Fig. 5. Thus, the critical pressure ratios of this study and the steady values compare extremely well for the major portion of these blowdowns. The transient, large duct, critical pressure ratios are somewhat greater than those for steady-state, small duct flow for entrance qualities greater than about 10 percent. However, this occurred reasonably late in these blowdowns after the most important segment of the decompressions had occurred. This was also when the homogeneous equilibrium predicted critical flow rate became similar in magnitude to the Henry-Fauske prediction [4]. This value of 10 percent entrance quality established in this transient, large duct experiment is precisely that observed in the steady-state, small duct case [4]. The internal vessel pressure started to decrease from its nearly constant value approximately when the homogeneous equilibrium critical flow rate agreed with the measured critical flow rate. This is consistent with the apparent occurrence of equilibrium of the remaining fluid, Fig. 2. The Moody model [5] significantly overpredicted the measured critical flow rates for the entire blowdown. The Henry-Fauske prediction [4] for the critical flow rate agreed well with the data while only being slightly greater than the measurements for most of the decompression.

The measured and calculated critical exit pressure ratios in tests 1 and 2 were also compared. The Henry-Fauske prediction of the overall critical pressure ratio history was best with both the homogeneous equilibrium and Moody predictions underestimating the data.

The measured and calculated remaining fluid mass within the blowdown vessel were also compared. The Moody prediction of the remaining fluid mass decreased very rapidly below the experimental results because of the excessively high predicted initial critical flow rate. The Henry-Fauske prediction of the remaining fluid mass followed the trend of the data reasonably well if not slightly underpredicting the measurements. The homogeneous equilibrium prediction of the remaining fluid mass was considerably greater than the data. This was because of the underprediction of the critical flow rate early in the blowdown.

The measured and calculated thrust histories in this experiment were also compared. The predicted thrust history obtained by employing the homogeneous equilibrium critical flow model in (12) agreed well with the data in the latter part of the decompression. However, the maximum in the predicted thrust history was later in time than the measurements indicated. This is due to the underpredicted critical flow rate early in the depressurization. The homogeneous equilibrium predicted thrust increased up to this time even with the underpredicted critical flow rate because of the increasing fluid quality, Fig. 4. The maximum thrust predicted by employing the Moody critical flow model in (12) was considerably greater than the measured maximum thrust. It was greater than the measured thrust for most of the blowdown except in the latter part of the decompression. The predicted maximum thrust obtained by using the Henry-Fauske critical flow model in (12) was only slightly greater than the measured maximum thrust. This prediction was also slightly greater than the measurements for most of the blowdown except in the latter period of the depressurization. However, it was less than the Moody prediction over the entire decompression.

Of the three cited critical flow analytical models, the measured histories in the blowdowns of this experiment were best predicted using the Henry-Fauske critical flow model.

4 Conclusions

The most significant conclusions drawn from the experimental portion of this study are as follows:

1 The fluid thermodynamic state inside the system during the blowdown is dependent on the internal vessel configuration. This is particularly pertinent at the start of blowdown from an initially subcooled or saturated liquid state. The primary vapor generation mechanism in such a system is predominately the activation and growth of bubbles originating from surface cavities. Vapor generation in the bulk liquid has not been shown to be significant. Thus, the ratio of internal vessel solid surface area to initial liquid volume is a useful criterion for assessing how quickly a dispersed, two-phase mixture is approached. The resulting local fluid compressibility greatly affects total pressure losses throughout the system and ultimately the critical flow rate from the break in the system.

2 The initial decrease of the internal vessel pressure at the start of blowdown occurs because the initial volume exhaust rate exceeds the vapor volume production rate. The initially retarded volume production rate (by bubble growth) is due to the metastable, superheated liquid state which is initially created and its subsequent relaxation toward thermodynamic equilibrium.

3 Choking only occurred at the exit of the exhaust duct in this system.

4 There was a significant nonuniform fluid quality distribution within this system early in these blowdowns. This was due to a lack of solid surface area per unit liquid volume inside the internal skirt region to aid in vapor phase generation. Hence, the liquid in the internal skirt region remained as a superheated liquid at the start of these decompressions. Once the fluid in this region became

dispersed, thermodynamic equilibrium was approached, and the internal vessel pressure began to decrease.

5 The Henry-Fauske critical flow model provides the best available prediction of the overall characteristics of the two phase decompression phenomenon observed in this experiment.

6 The two phase critical flow phenomenon is essentially the same in the transient, large duct and steady-state, small duct cases.

Acknowledgment

The authors acknowledge the financial support for this study from the United States Energy Research and Development Administration. This work was performed in the Experimental Modeling Section of the Reactor Analysis and Safety Division of Argonne National Laboratory.

References

1 Henry, R. E., Grolmes, M. A., and Fauske, H. K., "Pressure Drop and Compressible Flow of Cryogenic Liquid-Vapor Mixtures," *Heat Transfer at Low Temperatures*, edited by Walter Frost, ch. 11, Plenum Press, New York, 1975, p. 229.

2 Henry, R. E., Fauske, H. K., and McComas, S. T., "Two-Phase Critical Flow at Low Quality, Part I: Experimental," *Nuclear Science and Engineering*, Vol. 41, 1970, pp. 79–91.

3 Henry, R. E., Fauske, H. K., and McComas, S. T., "Two-Phase Critical Flow at Low Quality, Part II: Analytical," *Nuclear Science and Engineering*, Vol. 41, 1970, pp. 92–98.

4 Henry, R. E., and Fauske, H. K., "The Two-Phase Critical Flow of One Component Mixtures in Nozzles, Orifices, and Short Tubes," ASME JOURNAL OF HEAT TRANSFER, Vol. 93, No. 2, May 1971, pp. 179–187.

5 Moody, F. J., "Maximum Flow Rate of a Single Component, Two-Phase Mixture," ASME *Transactions*, Vol. 87, No. 1, Feb. 1965, p. 134.

6 Prisco, M. R., Henry, R. E., Hutcherson, M. N., and Linehan, J. L., "Nonequilibrium Critical Discharge of Saturated and Subcooled Liquid Freon-11," *Nuclear Science and Engineering*, Vol. 63, No. 4, Aug. 1977, pp. 365–375.

7 Sozzi, G. L., and Sutherland, W. A., "Critical Flow of Saturated and Subcooled Water at High Pressure," NEDO-13418, General Electric Co., San Jose, Calif., July 1975.

8 Fauske, H. K., "Some Ideas About the Mechanism Causing Two Phase Critical Flow," Appl. Sc. Res., Vol. 13, Section A, 1964, pp. 149–160.

9 Starkman, E. S., Schrock, V. E., Neusen, K. F., and Maneely, D. J., "Expansion of a Very Low Quality Two-Phase Fluid Through a Convergent-Divergent Nozzle," ASME *Journal of Basic Engineering*, Vol. 86, No. 2, June 1964, p. 247.

10 Shrock, V. E., Starkman, E. S., and Brown, R. A., "Flashing Flow if Initially Subcooled Water in Convergent-Divergent Nozzles," ASME JOURNAL OF HEAT TRANSFER, Vol. 99, May 1977, pp. 263–268.

11 Hutcherson, M. N., "Contribution to the Theory of the Two-Phase Blowdown Phenomenon," (*a*) ANL-75-82, Argonne National Laboratory, 1975: (*b*) And Interim Report, ANL/RAS 75-42, 1975: (*c*) Also, University Microfilms, 76-21951, 1976: (*d*) And University of Missouri, Mechanical Engineering Department, Ph.D. dissertation, Columbia, Mo. 1975.

12 Hutcherson, M. N., "Numerical Evaluation of the Moody Critical Flow Model," MDC N9653-110, McDonnell Douglas, St. Louis, Missouri, Sept. 1980.

13 Hutcherson, M. N., "Numerical Evaluation of the Henry-Fauske Critical Flow Model," MDC N9654-100, McDonnell Douglas, St. Louis Mo., July 1980.

14 Hutcherson, M. N., "Numerical Evaluation of the Homogeneous-Equilibrium Critical Flow Model," MDC N10437-041, McDonnell Douglas, St. Louis, Mo., Apr. 1981.

15 Hutcherson, M. N., "Numerical Evaluation of the Homogeneous Frozen Critical Flow Model," MDC N10438-041, McDonnell Douglas, St. Louis, Mo., Apr. 1981.

16 Wallis, G. B., "Critical Two-Phase Flow," *International Journal of Multiphase Flow*, Vol. 6, No. 1–2, Feb.-Apr. 1980, pp. 97–112.

17 Henry, R. E., "Two-Phase Compressible Flow," *EPRI Workshop Proceedings: Basic Two Phase Flow Modeling in Reactor Safety and Performance*, Vol. 2, Tampa, Fla., Feb. 27–Mar. 2, 1979, pp. 9-67:9–106.

18 Hutcherson, M. N., Henry, R. E., and Gunchin, R. R., "Compressible Aspects of Water Reactor Blowdown," *Transactions ANS*, Vol. 18, 1974, p. 232.

19 Hutcherson, M. N., Henry, R. E., and Wollersheim, D. E., "Experimental Measurements of Large Pipe Transient Blowdown," *Transactions ANS*, Vol. 20, Paris, France, Apr. 21–25, 1975, pp. 488–490.

20 Hutcherson, M. N., Henry, R. E., and Wollersheim, D. E., "The Two-Phase Blowdown Phenomenon in a Small LWR Geometry," *Transactions ANS*, Vol. 22, San Francisco, Calif., Nov. 16–21, 1975, pp. 466–467.

21 Hutcherson, M. N., Henry, R. E., and Wollersheim, D. E., "Two-Phase Vessel Blowdown of an Initially Saturated Liquid, Part 2-Analytical, ASME JOURNAL OF HEAT TRANSFER, Vol. 105, No. 4, pp. 694–699.

22 Morrison, A. F., "Blowdown Flow in the BWR BDHT Test Apparatus," GEAP-21656, NRC-2, General Electric Co., San Jose, Calif., 1977.

23 Hall, D. G., "A Study of Critical Flow Prediction for Semiscale Mod-1-Loss-of-Coolant Accident Experiments," TREE-NUREG-1006, EGG, Idaho, 1976.

24 Bayless, P. D., Marlow, J. B., and Averill, R. H., "Experimental Data Report for LOFT Nuclear Small Break Experiment L3-1," EGG-2007, NUREG/CR-1145, EGG, Idaho, Jan. 1980.

25 Hall, D. G., "An Evaluation of the Accuracy of Five Critical Flow Models Using Transient Data," *Proceedings of the Topical Mtg. on Thermal Reactor Safety*, CONF-770708, Sun Valley, Id., 1977, pp. 2–493.

26 Martinec, E. L., "A Comparison of the Marviken Critical Flow Tests With the Henry-Fauske Model," ANL/RAS/LWR 79-8, Argonne National Laboratory, Argonne, Ill., Dec. 1979.

27 Winters, W. S., and Merte, H., "Experiment and Nonequilibrium Analysis of Pipe Blowdown," Nucl. Sci. and Eng., Vol. 69, 1979, pp. 411–429.

28 Weisman, J., Bussell, G., Jacknani, I. L., and Hsieh, T., "The Initiation of Boiling During Pressure Transients," ASME Paper No. 73-WA/HT-25, 1973.

29 Hooper, F. C., and Abdelmessih, A. H., "The Flashing of Liquids at Higher Superheats," *Proceedings 3rd Intl. Heat Transfer Conf.*, Chicago, Ill., Vol. 4, Aug. 1966, pp. 44–50.

30 Hooper, F. C., Faucher, G., and Eidlitz, A., "Pressure Effects on Bubble Growth in the Flashing of Superheated Water," *Proceedings 4th Int. Heat Transfer Conf.*, Vol. 5, Paper No. B2.3, Paris-Versailles, France, 1970.

31 Kenning, D. B. R., and Thirunavukkarasu, K., "Bubble Nucleation Following a Sudden Pressure Reduction in Water," *Proceedings 4th Intl. Heat Transfer Conf.*, Vol. 5, Paper B2.9, Paris-Versailles, France, 1970.

32 Hoppner, G., "Experimental Study of Phenomena Affecting the Loss of Coolant Accident," Ph.D., thesis, University of California at Berkeley, 1971.

33 Radovcich, N. A., and Moissis, R., "The Transition from Two-Phase Bubble Flow to Slug Flow," MIT Report 7-7673-22, 1962.